

Black Holes in the Early Universe

Marta Volonteri^{1,2}, Jillian Bellovary²

¹Institut d'Astrophysique de Paris, Paris, France

²University of Michigan, Ann Arbor, MI, USA

E-mail: martav@iap.fr; jillianx@umich.edu

Abstract.

The existence of massive black holes was postulated in the sixties, when the first quasars were discovered. In the late nineties their reality was proven beyond doubt, in the Milky way and a handful nearby galaxies. Since then, enormous theoretical and observational efforts have been made to understand the astrophysics of massive black holes. We have discovered that some of the most massive black holes known, weighing billions of solar masses, powered luminous quasars within the first billion years of the Universe. The first massive black holes must therefore have formed around the time the first stars and galaxies formed. Dynamical evidence also indicates that black holes with masses of millions to billions of solar masses ordinarily dwell in the centers of today's galaxies. Massive black holes populate galaxy centers today, and shone as quasars in the past; the quiescent black holes that we detect now in nearby bulges are the dormant remnants of this fiery past. In this review we report on basic, but critical, questions regarding the cosmological significance of massive black holes. What physical mechanisms lead to the formation of the first massive black holes? How massive were the initial massive black hole seeds? When and where did they form? How is the growth of black holes linked to that of their host galaxy? Answers to most of these questions are work in progress, in the spirit of these Reports on Progress in Physics.

1. Overview: Evidences and Constraints on Black Holes in the First Galaxies

Since the discovery of Sagittarius A* (Balick & Brown 1974), evidence has been growing that all massive galaxies host massive black holes (MBHs) in their centers. As our observing power has increased, we have seen how these MBHs can exist as powerful quasars, capable of discharging prodigious amounts of energy. Over time, we have formed a picture where MBHs and their host galaxies co-exist and co-evolve. Galaxies build up their mass through accretion and mergers, and during these events MBHs build up their mass as well, undergoing periods of activity and quiescence (Croton et al. 2006, Bower et al. 2006). An apparent result of this hierarchical buildup is the observed relation between the host galaxy spheroid and the MBH mass. This relation holds whether one measures the spheroid's velocity dispersion[‡] (Ferrarese &

[‡] The velocity dispersion is the root mean square of stellar velocities, and it gives a measure of the motion of stars under the effect of the galaxy potential.

Merritt 2000, Gebhardt et al. 2000, Tremaine et al. 2002, Gültekin et al. 2009), mass (Magorrian et al. 1998, Häring & Rix 2004), luminosity (Marconi & Hunt 2003), or other host properties (such as number of globular clusters (Burkert & Tremaine 2010) and their global velocity dispersion (Sadoun & Colin 2012) or the Sersic index (Graham & Driver 2007)).

To determine how these relationships (and MBH growth and evolution in general) have arisen, we must look to the early universe. The discovery of quasars at $z \sim 6$ demonstrates that MBHs must form extremely early on and grow rapidly in order to acquire $10^9 M_{\odot}$ of mass within a span of ~ 1 Gyr (Fan et al. 2001). How effectively MBH growth proceeds from their ‘seeds’ is hard to gauge, as most current observations are sensitive only to the most luminous quasars ($L > 10^{44}$ erg/s), hence the most massive MBHs ($M_{BH} > 10^{8-9} M_{\odot}$). Recent attempts at investigating lower luminosity sources have provided conflicting results. While (Treister et al. 2011) suggested that the vast majority of high redshift MBHs may be obscured and accreting rapidly, hinting that much of MBH growth may be hidden from view, (Willott 2011), (Cowie et al. 2012) and (Fiore et al. 2012) do not find a population of obscured low-luminosity Active Galactic Nuclei (AGN).

As we expand our depth and wavelength coverage of the universe, we can use the evolving luminosity functions of quasars and galaxies to constrain MBH activity, and the link between MBHs and their hosts. Several groups have found evidence for “downsizing,” in which the peak of quasar activity was dominated by brighter, more massive MBHs at higher redshifts (Croom et al. 2009, Willott et al. 2010, Assef et al. 2011, Glikman et al. 2011). Such a pattern also reflects that of star formation activity (Cowie et al. 1996, Kodama et al. 2004, Treu et al. 2005, Bundy et al. 2006), and strengthens the argument that MBH activity and star formation/galaxy growth are interconnected.

In section 2 we will discuss the potential physical mechanisms which may form MBHs, and how future observations may aid us in determining the actual formation pathway. In section 3 we describe the numerous ways in which MBHs are interconnected with their host galaxies. Section 4 chronicles the current status of cosmological simulations, which are a crucial tool for exploring the entire co-evolutionary history of MBHs and their hosts. Finally, in section 5 we summarize with some open questions in the field and the future outlook of each.

2. The Physics of Black Hole Formation

As discussed in the previous section, MBHs with masses of $10^9 M_{\odot}$ have been identified at distances corresponding to a light travel time of more than 12 billion years. This means that these MBHs, as massive as the most massive black holes we detect in today’s galaxies, were in place when the Universe was less than one billion years old. One can easily understand why this is a significant feat by estimating the growth time of an MBH. Typically it is assumed that MBHs cannot accrete at rates much higher than permitted

by the ‘‘Eddington limit’’, which occurs when the luminosity of a source becomes large enough that radiation pressure overcomes gravity. Above the Eddington limit, material is pushed away instead of falling towards the black hole to fuel activity. The Eddington luminosity can be written as $L_{\text{Edd}} = M_{\text{BH}}c^2/t_{\text{Edd}}$, where $t_{\text{Edd}} = \frac{\sigma_T c}{4\pi G m_p} = 0.45 \text{ Gyr}$ (here c is the speed of light, σ_T is the Thomson cross section, and m_p is the proton mass). Therefore, if the inflow rate of mass towards the MBH is \dot{M}_{in} , and \dot{M} is the mass that goes into increasing the MBH mass, from:

$$L = \epsilon \dot{M}_{\text{in}}c^2 = L_{\text{Edd}}c^2 \quad (1)$$

and $dM = (1 - \epsilon)dM_{\text{in}}$, where $\epsilon \simeq 0.1$ is the efficiency of conversion of rest-mass into energy. The growth time of an MBH with initial mass M_0 is

$$t_{\text{growth}} = t_{\text{Edd}} \frac{\epsilon}{1 - \epsilon} \ln \left(\frac{M_{\text{BH}}}{M_0} \right). \quad (2)$$

For MBHs to reach $10^9 M_\odot$ within 1 Gyr, they must form early on and grow very rapidly (Haiman & Loeb 2001). To accomplish this, it is helpful if they form with an ‘‘intermediate’’ mass – M_0 between $100 - 10^5 M_\odot$ or so. A black hole of $1 M_\odot$ may grow 9 orders of magnitude in slightly over 1 Gyr only if it accretes at the Eddington rate for its entire lifetime; if feedback effects from stars and the MBH are negligible this growth may be possible, but such a scenario is extremely unlikely.

The key to forming an MBH seed at high redshift is obtaining the rapid collapse of ‘baryons’. Stars and gas represent the baryonic content of galaxies, to be contrasted with non-baryonic dark matter that does not interact radiatively, but only gravitationally with its environment. In the standard picture, the mass content of the Universe is dominated by cold dark matter, with baryons contributing at a 10% level only. Starting from a Gaussian density fluctuation field in a quasi-homogeneous Universe, dark matter perturbations grow to the point they collapse and virialize forming self gravitating halos within which gas eventually condenses to form the luminous portion of galaxies, comprising both gas and stars formed out of this gas. Normally, during the formation of galaxies part of the gas cools and becomes dense enough that gas clouds ‘‘fragment’’ into clumps where stars eventually form.

In the event of a rapid collapse of gas, which represents one of the possible starting points for MBH formation, some mechanism must be in place to prevent fragmentation into small clumps (and subsequent star formation). If fragmentation is prevented, most of the gas is actually funneled to forming the black hole, and the resulting object is massive. If the baryons are predominantly stellar objects, they must be able to merge in an efficient way without ejecting significant mass from the system. In all cases, the effects of feedback from accretion onto the MBH or nearby star formation will surely play a role in how massive the MBH can become before its growth is limited by its environment. In the following sections we review several proposed formation scenarios for MBH seeds and discuss the physical implications of each.

2.1. Population III Stars

For several years, the most promising mechanism to form MBHs at high redshift was assumed to be via the remnants of the very first generation of stars (Madau & Rees 2001). The first bout of star formation must occur, by definition, when gas still had primordial composition (i.e., all the atoms heavier than hydrogen were produced through primordial nucleosynthesis, and heavy elements, globally defined as “metals” in astrophysics, were absent). These stars are commonly referred to as Population III, or Pop III, stars. Such stars have been speculated to have formed with masses much larger than today’s stars, so that the typical mass of a Pop III star would be hundreds of solar masses (Couchman & Rees 1986, Abel et al. 2002, Bromm & Larson 2004). In particular, if stars of primordial composition existed with masses greater than $260 M_{\odot}$, they are predicted to directly collapse into a black hole of $\sim 100 M_{\odot}$ (Bond et al. 1984, Heger & Woosley 2002).

Recent simulation results have put this picture into question. The inclusion of more complex physics combined with higher resolution has resulted in models of Pop III stars with lower masses. (Turk et al. 2009) showed that fragmentation may be common in Pop III star collapse, and thus Pop III binaries with masses of a few tens of M_{\odot} could be fairly run-of-the-mill. Improvements in simulation techniques such as the addition of turbulence (Clark et al. 2011), radiative feedback (Stacy et al. 2012), or entirely new codes (Greif et al. 2011) have confirmed this result, showing that Pop III stars may form in binaries and/or clusters with a wide range of initial masses (though primarily in the 10-100 M_{\odot} range, probably). The existence of a large number of isolated stars with masses larger than $260 M_{\odot}$ has thus been called into doubt. While the remnants of stars with masses less than $140 M_{\odot}$ might still become MBH seeds, these objects form in shallow potential wells which are unable to retain photoionized heated gas. and may be starved of accretable gas for a local Hubble time (Johnson & Bromm 2007). Massive Population III binaries may be able to fuel an existing MBH via binary accretion/ejection and subsequent tidal disruption (see (Bromley et al. 2012)), but the central stellar density may not be large enough for this process to be efficient until a large number of stars have formed (in simple models the event rate scales linearly with the central stellar density, but see (Merritt 2009) and references therein for detailed calculations). Models which predict the evolution of Pop III seeds into today’s MBH population (i.e. (Volonteri et al. 2003)) assume that a substantial fraction of Pop III stars form MBH seeds. The potential rarity of Pop III MBH seeds combined with their smaller size makes them rather unattractive candidates for being the precursors to $z = 6$ quasars.

2.2. Direct Collapse and Quasi-Stars

Several works have recently discussed how a rapid inflow of gas may collapse to form an MBH directly (Loeb & Rasio 1994, Eisenstein & Loeb 1995, Oh & Haiman 2002, Bromm & Loeb 2003, Koushiappas et al. 2004, Begelman et al. 2006, Lodato & Natarajan 2006, Begelman et al. 2008). Such a phenomenon can only occur if the gas does not fragment,

but instead undergoes larger-scale dynamical instabilities. Preventing fragmentation generally requires inhibiting cooling, either by requiring no metals and/or preventing the formation of H_2 via a substantial Lyman-Werner background. In addition, the gas must have low intrinsic angular momentum, so that it may reach the halo center without being inhibited by the formation of a rotationally supported disk. In low-angular momentum halos, the disk will be compact, and gravitational instabilities are able to occur. These instabilities are responsible for rapidly funneling gas inwards (and angular momentum outwards).

Global dynamical instabilities, such as the “bars within bars” instability, may act to repeatedly transport gas inwards on the order of a dynamical time (Begelman et al. 2006). Alternatively, large-scale torques from major merger activity may be the driver of rapid gas inflow (Mayer et al. 2010). In such a case, turbulence may be the inhibitor of fragmentation, and the requirement of metal-free gas may be relaxed (see also (Begelman & Shlosman 2009)).

Local dynamical instabilities are instead described through the Toomre criterion:

$$Q_c = \sqrt{2} \frac{c_s V_h}{\pi G \Sigma R} \quad (3)$$

where c_s is the sound speed of the gas, V_h is the circular velocity of the disk, Σ is the surface density of the disk, and R is the cylindrical radial coordinate. When Q_c approaches a value of an order unity, the disk becomes unstable and fragments. This process is expected to occur in halos with a virial temperature of $T_{vir} \sim 10^4$ K, which are likely metal-free and do not contain molecular hydrogen. In such halos, fragmentation is suppressed, cooling proceeds gradually, and the gaseous component can cool and participate in MBH formation before it is turned into stars (Lodato & Natarajan 2006). These halos may need to exist in regions of ultracritical UV radiation in order to form MBHs by direct collapse (Dijkstra et al. 2008, Shang et al. 2010), since the average estimated UV background may not be sufficient to prevent some Pop III stars from forming in halos of this size (Johnson et al. 2008).

In general the step between “gas infall” and black hole formation has been dodged, and generic “post-Newtonian instabilities” have been advocated for converting the infalling gas into an MBH seed. An exception is the picture proposed by (Begelman et al. 2006), which can emerge in case of very high gas infall rates, exceeding about $1 M_\odot \text{ yr}^{-1}$. In this case, the collapsing gas traps its own radiation and forms a quasistatic, radiation pressure-supported supermassive star, which burns hydrogen for about a million years while growing to a mass $\sim 10^6 M_\odot$ (Begelman et al. 2006, Begelman 2010) before its core collapses and forms a black hole. This black hole is surrounded by the massive envelope created by the inflow, and it can grow rapidly at a rate set by the Eddington limit for the massive gaseous envelope, thus accreting at several hundred to thousand times its own Eddington rate without violating the luminosity criterion. The resulting object, comprising a growing MBH embedded in a radiation-pressure supported envelope, dubbed a ‘quasistar’, resembles a red giant star with a luminosity comparable to an AGN. As the black hole grows inside it, its photosphere expands and

cools until it hits a minimum temperature associated with the Hayashi track, at which point it disperses, leaving behind the naked seed MBH with a mass of thousands to hundred thousands of solar masses.

2.3. Collapsing Clusters

Stellar-dynamical processes may also have a role in creating MBH seeds at high redshift. In many cases, galaxies which host MBHs also host nuclear star clusters (Seth et al. 2008, Graham & Spitler 2009). While the link between these nuclear objects is not fully understood, one can easily imagine a scenario where a central cluster undergoes core collapse and forms a single massive compact object at its center.

(Devecchi & Volonteri 2009) postulate that such a scenario is likely if a nuclear cluster forms out of the second generation of stars in a galaxy, when the metallicity (i.e., the heavy element content) of the gas is still very low, of order $10^{-5} - 10^{-4}$ the metallicity of the Sun (see also (Omukai et al. 2008)). At sub-solar metallicity, the mass loss due to winds is much more reduced in very massive stars, which greatly helps in increasing the mass of the final remnant. In Toomre-unstable proto-galactic discs, instabilities lead to mass infall instead of fragmentation into bound clumps and global star formation in the entire disk. The gas inflow increases the central density, and within a certain compact region star formation ensues and a dense star cluster is formed. At metallicities $\sim 10^{-5} - 10^{-4}$ solar, the typical star cluster masses are of order $10^5 M_{\odot}$ and the typical half mass radii ~ 1 pc \S (Devecchi et al. 2010, Devecchi et al. 2012). Most star clusters can go into core collapse in ~ 3 Myr, and runaway collisions of stars form a very massive star, leading to an MBH remnant with mass $\sim 10^3 M_{\odot}$.

A scenario which invokes no dependence on metallicity or redshift has been proposed by (Davies et al. 2011). If the rapidly inflowing gas scenario (as mentioned above) occurs in a system where there is a pre-existing dynamically segregated nuclear cluster, the potential well of the cluster will deepen rapidly. In such a situation, the timescale for collapse of the the compact objects at the core of the cluster will be shorter than the timescale for dynamical heating via binaries. The binding energy of the cluster will be large enough that recoiling or dynamically ejected objects are actually retained. The result is a runaway collapse of compact cluster objects which may form an MBH of $10^5 M_{\odot}$ at high redshift.

2.4. Other Models

Primordial black holes may also be formed in the early universe before the epoch of galaxy formation (Carr 2003, Khlopov 2010) in regions where high density fluctuations are large and the whole region can collapse and form a primordial black hole. Generically, primordial black holes are formed with masses that roughly equal the mass within the particle horizon at the redshift of their formation (Zel'Dovich &

\S A parsec is a unit of measure of distance corresponding to a parallax of one second. It corresponds to 3.26 light-years or 3.1×10^{18} cm.

Novikov 1967, Hawking 1971). The masses of primordial black holes therefore range roughly from the Planck Mass (black holes formed at the Planck epoch) to $\simeq M_{\odot}$ (black holes formed at the QCD phase transition) up to $10^5 M_{\odot}$ (Khlopov et al. 2005).

Several physical or astrophysical constraints restrict the mass range where primordial black holes are allowed. Primordial black holes with an initial mass smaller than about 5×10^{14} g are expected to have already evaporated due to Hawking radiation. For masses $\sim 10^{15}$ g, there are strong bounds from the observed intensity of the diffuse gamma ray background (Page & Hawking 1976), limiting their contribution to the matter density to less than one part in 10^8 . For larger masses, constraints can be deduced from microlensing techniques (Alcock et al. 2000, Tisserand et al. 2007) and from spectral distortions of the cosmic microwave background (Ricotti et al. 2008) which limit the mass to below $\sim 10^3 M_{\odot}$.

2.5. Observational perspectives.

Directly observing the MBH formation process must wait for the launch of low-frequency gravitational wave detectors (e.g., eLISA, ET- Einstein Telescope) or until the next generation of telescopes (or perhaps the generation after that). To determine which (if any) of the seed models is correct, detailed population modeling is required. The primary parameters which characterize each seed model are formation redshift, initial mass, and the efficiency of formation. In addition, one must consider subsequent effects that affect an MBH's evolution, such as the growth for extended periods of time that affects MBHs over the cosmic history, thus erasing information on the original seed mass, or how central MBH populations are affected by ejections due to gravitational recoil during MBH mergers, thus erasing information on the efficiency of MBH formation. The list of unknowns is large, but we can explore each of them in turn and hope to constrain MBH populations vis a vis various seed models.

For example, (van Wassenhove et al. 2010) investigate the evolution of MBHs in a Milky Way-like galaxy with two seed formation models – one resembling Pop III stars and one resembling direct collapse. The main difference between the models is effectively the mass of the seeds and the formation efficiency, as massive seeds require larger halo masses with specific angular momentum criteria compared to low-mass seeds. The left panel of Figure 1 shows the occupation fraction of MBHs (top), i.e., how many galaxies host an MBH, for various Pop III models (green) and the direct collapse model (red). This figure exemplifies where we may find a trace of the MBH formation mechanism: at low galaxy mass. While large systems always host MBHs in either case, the Pop III model exhibits a larger occupation fraction at smaller masses, due to the larger number of Pop III black holes formed in the early universe with respect to the direct collapse case. An effect is seen in the MBH-host galaxy relation as well; MBHs lurk in low mass galaxies but do not undergo any significant growth over their lifetimes. The mass of MBHs today is still very close to the original seed mass (bottom). These objects exist as intermediate mass black holes hiding in dwarf galaxies, and are unlikely to be observed

because of their extremely low predicted accretion rates, and their tiny dynamical region of influence.

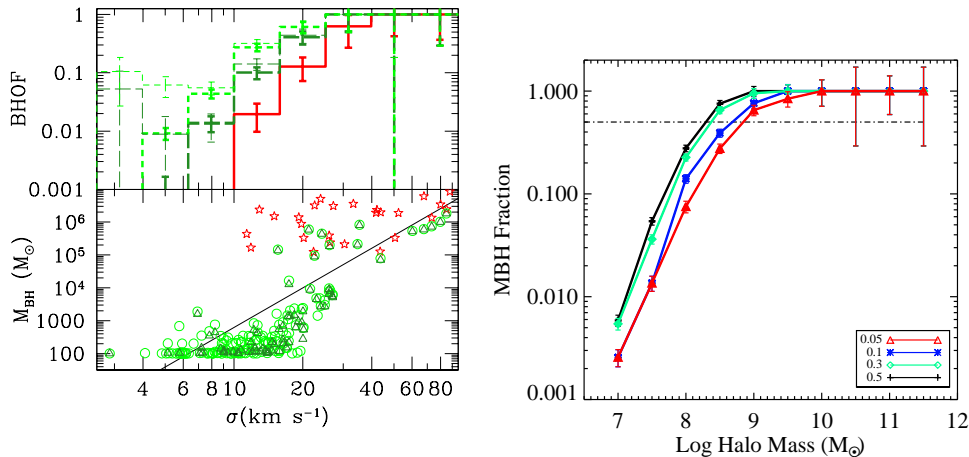


Figure 1. Left: Occupation fractions and the correlation of MBH mass and host velocity dispersion, σ , are different with different MBH formation models. Taken from (van Wassenhove et al. 2010). Right: The MBH-halo occupation fraction for a given halo mass at $z = 5$ in cosmological simulations. Colored lines and symbols represent simulations with different values of the efficiency of MBH formation (Bellovary et al. 2011). Reproduced by permission of the AAS

A critical question for MBH seed formation is therefore “how many dwarf galaxies host MBHs?” While the answer currently appears to be “very few,” one must keep in mind that such objects would be extremely difficult to observe. Gas surface densities are low in dwarfs, so accretion rates would be extremely small, even taking into account gas lost from stars (Volonteri et al. 2011). The surface density of stars is also quite low, so detecting MBHs using stellar dynamics is challenging given that there are so few stars in the radius of influence (van Wassenhove et al. 2010). In some cases, such as the Large Magellanic Cloud, the dynamical center is not well constrained, so it is unclear where we should look to find an MBH. Since dwarf galaxies exhibit cored density profiles, the MBH may not even inhabit the exact center of the galaxy, but may “slosh” around within the central core region. Given these challenges, only a few dwarf galaxies have been found to host AGN. For example, the dwarf elliptical Pox 52 (Barth et al. 2004) and the dwarf irregular Henize 2-10 (Reines et al. 2011) each host an MBH of around 10^5 and $10^6 M_{\odot}$, respectively.

The occupation fraction of MBHs in galaxies is a key clue to the mechanism of seed formation. In cases where the formation efficiency of MBH seeds is high, one expects to find seeds in a larger fraction of galaxies, regardless of whether these seeds have grown into SMBHs. Such an effect is indeed seen in cosmological simulations where seed formation efficiency is varied (Bellovary et al. 2011) (Figure 1, right). Observing the MBH halo occupation is challenging, because for the most part we can only observe *active* black holes in galaxies. Still, measuring the active fraction of MBHs in galaxies

provides a lower limit on the MBH occupation fraction. Nuclear activity due to MBHs has been detected in 32% of the late-type galaxies in the Virgo Cluster, exclusively in galaxies with mass $M_{halo} > 10^{10} M_{\odot}$ (Decarli et al. 2007). For early-type galaxies in Virgo, nuclear activity exists in 3-44% of galaxies with mass less than $10^{10} M_{\odot}$, and 49 - 87% of galaxies with mass greater than $10^{10} M_{\odot}$ (Gallo et al. 2008). A similar study of early-type field galaxies gives an occupation fraction of $45 \pm 7\%$ (Miller et al. 2012). Further studies will need to extend down to lower mass galaxies as well as higher redshifts. Data at $z \sim 1$ from DEEP2 and AEGIS may help provide some constraints (see (Yan et al. 2011)).

3. The Interplay Between Black Holes and Their Host Galaxies

Today's MBH masses are found to scale with the properties of their hosts, as described in the Introduction, thus determining MBH - host scaling relations (e.g., Fig. 2, left). These relations extend over several orders of magnitude in MBH mass, though scatter does increase at both the low and high mass ends (Gültekin et al. 2009, Greene et al. 2010, McConnell et al. 2011). It is also not entirely clear what sets this relationship: is it a connection between the MBH and the stellar properties of the bulge? Or, is the driving property the global potential well of the galaxy, or even the host dark matter halo?

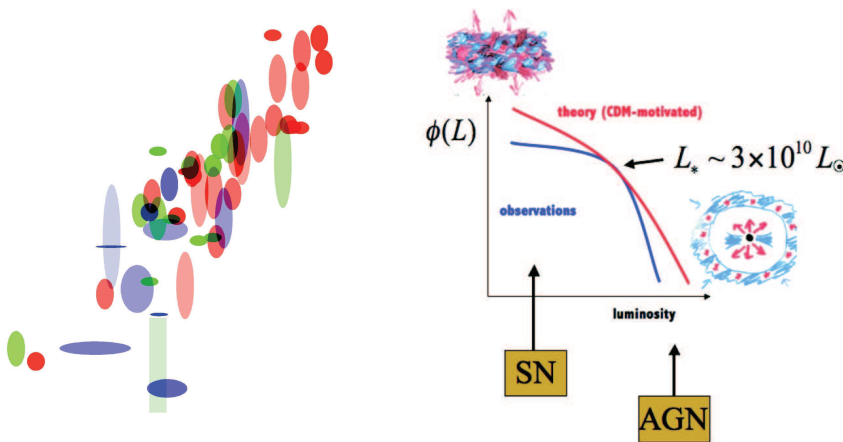


Figure 2. Left: the masses of MBHs in nearby galaxies are found to scale with many properties of the host galaxies, including the velocity dispersion, as shown here. Figure taken from (Gültekin et al. 2009). Reproduced by permission of the AAS. Right: cartoon depicting how we think that different types of feedback affect the relationship between galaxies and dark matter halos. Supernovae are believed to be responsible for limiting the formation of stars in small galaxies, while AGN feedback is suggested to be shutting off star formation in large galaxies. Figure taken from (Silk 2011).

Studying MBH scaling relations at higher redshifts may help understanding how the relationships are established, but measurements are fraught with difficulty. Current studies yield mixed results, with several authors finding that at high z MBHs are more

massive for a given velocity dispersion (Peng et al. 2006, Woo et al. 2008, Bennert et al. 2011, Targett et al. 2012), but others finding the opposite (Alexander et al. 2008) or no evolution at all (Sarria et al. 2010). Part of the difficulty in deciphering the data is the difficulty of obtaining reliable MBH mass estimates. Robust methods that are used in the local universe (i.e. dynamical measurements, reverberation mapping) are not possible for more distant objects. MBH masses must be estimated using broad line widths; at higher redshifts, different lines must be used for this measurement, and the correlation between masses derived by $H\alpha$, C IV and Mg II has a large amount of scatter (Greene et al. 2010). Bulge velocity dispersion measurements are straightforward for nearby galaxies, but at higher redshifts a bulge mass or luminosity estimate becomes much more difficult due to surface brightness dimming, inclination effects, and dust extinction. These difficulties are compounded with the selection effects inherent in the large surveys which are used for target selection. If our surveys are simply picking out objects which are the most luminous, and in turn have the highest masses for a given host property, the MBH-host relations will appear to evolve toward more massive MBHs at higher redshift – a type of Malmquist bias (Lauer et al. 2007). These factors compounded make observational determinations of the evolution of the MBH scaling relations extremely challenging (Volonteri & Stark 2011).

While MBHs are harbored in the central regions of their galaxies, evidence is mounting that their mere existence can affect a number of larger-scale galaxy properties. The primary culprit is postulated to be feedback, or the effect of the energy released upon gas accretion by the MBH (Silk & Rees 1998). Numerous studies have reported on the repercussions of *stellar* feedback (Murray et al. 2005, Oppenheimer & Davé 2008, Hopkins et al. 2011) and it should not be surprising that MBHs may act similarly. In fact, AGN feedback has been advocated as a solution for the underabundance of star forming galaxies with respect to many predictions of theoretical models of galaxy formation, making ellipticals “red and dead” (Croton et al. 2006, Schawinski et al. 2007). The discrepancy between the simulated halo mass function and the observed galaxy luminosity function is perhaps the best demonstrator of feedback effects. In Figure 2 (right), we can see that the two curves diverge at low and high masses. The low-mass divergence is postulated to be caused by stellar feedback; supernova winds drive baryons out of small galaxies fairly efficiently, but as galaxies become larger the winds do not have enough energy to escape the potential well. At high galaxy masses, AGN feedback may be strong enough to transport baryons out of massive halos. This loss of baryons decreases the star forming potential of a galaxy, hence the divergence in the luminosity function from the halo mass function. Observationally, however, the situation appears much more complex. In the host galaxies of moderate-luminosity AGN, star formation typically precedes MBH accretion, suggesting that in early phases supernova feedback may suppress MBH growth (Schawinski et al. 2009, Davies et al. 2007), or that mass loss from newly formed stars is what fuels MBHs (Ciotti & Ostriker 2007, Wild et al. 2010). Further explorations of how MBHs are fueled, and how star formation and AGN activity are linked on small scales (Davies et al. 2004) or along cosmic history

(Mullaney et al. 2012), are needed before the complex interplay of MBHs and their hosts is understood.

Another observed consequence of MBH feedback and its effect on a host galaxy is AGN winds. Such winds are observed on all scales, from very close to the MBH in broad absorption line quasars, to galaxy-wide distances (e.g. (Tremonti et al. 2007)). These outflows cause the transport of gas from the galaxy center to its halo, or possibly out of the system entirely. For example, (Nesvadba et al. 2008) observed three quasars with radio jets at $z \sim 2 - 3$ and found outflow velocities of 800-1000 km s⁻¹ and ionized gas masses on the order of $10^{10} M_{\odot}$. Molecular AGN-powered outflows have been detected in more local galaxies by (Feruglio et al. 2010, Alatalo et al. 2011), who find that the mass outflow rate is enough to deplete the molecular gas reservoir in about a dynamical time. Clearly such a rapid gas mass loss will drastically affect the evolution of a galaxy. Determining how much gas is lost and how quickly is a complex question of AGN luminosity, gas properties, and the mechanism of the energy coupling to the gas. These questions are non-trivial and cannot be generalized; a full range of parameter space must be explored in simulations and observations in order to make headway here.

4. Modeling Black Holes and Galaxies in a Cosmological Context

In order to capture the evolutionary process of MBHs from their birth to the present day, one must embed the physics of MBHs in a cosmological setting. Cosmological simulations are key for tracing MBH and galaxy populations throughout their lifetimes, gaining meaningful statistics, and exploring the main drivers of their evolution.

4.1. Semi-Analytical Models

Analytical models of MBH formation and evolution have been developed as described in sections 2 and 3. These models have been embedded in so-called semi-analytical models of galaxy formation. Semi-analytical codes study the evolution of the baryonic content of galaxies (gas, stars, black holes) upon a skeleton given by the dark matter halo merger history, which can be extracted from N-body cosmological simulations, or built through Monte Carlo techniques, given initial conditions (cosmological parameters, power spectrum of density fluctuations). Semi-analytical techniques are based on physically motivated recipes, which describe the physical processes occurring during the evolution of galactic structures. For instance, one can compute several properties of the MBH population, given by the combination of the birth rate, death rate (MBH-MBH mergers), and accretion rate on each MBH. The latter provides a duty cycle for the active MBHs (quasars and AGNs). The code requires that we specify physical properties for the evolving galaxies and MBHs, e.g., density profiles of halos and galaxies, accretion rate onto MBHs (e.g., Eddington, Bondi), accretion disc properties (e.g., Shakura–Sunyaev), and what the triggers for accretion and its termination are (e.g., galaxy mergers, feedback on the host). We also need to specify the physical laws governing the

evolution of MBH binaries (e.g., dynamical friction, stellar dynamical equations). As an example (Volonteri et al. 2003, Volonteri et al. 2008, Volonteri & Begelman 2010) models are based on comprehensive set of quantities of theoretical interest, outlined in the scheme below.

Input: \rightarrow - Cosmology - Galaxy properties: density profiles, dynamical friction, stellar dynamical equations - Accretion properties: Eddington ratio, Spectral energy distribution	Modelization: \rightarrow - MBH birth rate - MBH merger rate - MBH ejection rate - Growth rate - Duty cycle	Observables: - AGN LF at $z \geq 0$ - AGN redshift distributions - MBHs mass functions - Occupation fraction of MBHs - LISA event rates, masses, z - X-ray background
--	--	---

The theoretical properties can be cast in terms of *observables* to be tested against current and future data. For each model we can calculate Luminosity Functions (LFs), number counts and redshift distributions of AGN at different redshifts and wavelengths, contribution to cosmic backgrounds, and event rates for gravitational wave detectors. The input parameters of semi-analytical models are very similar to those of hydrodynamical simulations, as described in section 4.2.

Semi-analytical models are very efficient and provide an excellent insight to physical mechanisms, allowing to explore a large parameter space in short computational times. The main weakness of semi-analytical models is the lack of spatial information (except for the code PINOCCHIO, that uses Lagrangian techniques to derive the spatial relationship between merging halos as well (Monaco et al. 2002)), the necessity of sticking to a rigid scheme that applies to all systems in the sample, and the inability of modeling systems that do not have smooth, analytical properties (e.g., galaxy mergers). The main advantages of semi-analytical models is that they are very efficient and provide an excellent insight to physical mechanisms, allowing to explore a large parameter space in short computational times. Because of the extremely high computational cost, in fact, cosmological simulations do not allow for extended parameter space exploration or large volume sampling at high spatial resolution (Springel et al. 2005, Di Matteo et al. 2008).

4.2. Numerical Simulations

The ability to self-consistently model halo growth, gas accretion, star formation, feedback processes, hydrodynamics, and MBH activity makes these models the most sophisticated theoretical tool we have to explore galaxy and MBH evolution. Of course, there are also limitations to this method; the need to model substantial volumes with a large dynamic range limits the spatial and mass resolution, and specific models of how, e.g., stars form and explode as supernovae, or MBH form and accrete must be implemented as “sub-grid” physics, as they cannot be explicitly resolved. To give a sense of the problem, the size of the disc of the Milky Way is tens of kpc, and our galaxy is embedded in a dark matter halo of size \sim Mpc. The scale of the region where an MBH dominates gravity is \sim tens of pc. The event horizon (Schwarzschild radius)

of an MBH is of order μpc scale. Therefore if one wanted to resolve the plunge of particles into an MBH in a galaxy like the Milky Way would need a dynamical range of 12 orders of magnitude. On scales of the event horizon, additionally, simulations would require full general relativity. Finally, the difference in timescales between galaxies and MBHs translates into enormously different required timesteps. While on galactic scales timescales are of order of at least $10^4 - 10^5$ yrs, close to the horizon of a BH timescales are of order of days or hours, as material moves close to the speed of light. This said, one attempts to capture as well as possible the most important physical mechanisms to understand the formation and evolution of MBHs in a cosmological setting.

4.2.1. Seed Formation. The first generation of cosmological smoothed particle hydrodynamics (SPH) simulations placed one MBH in the center of each massive galaxy by running an on-the-fly halo finder and identifying halos with a predetermined threshold mass (usually 10^9 or $10^{10} M_{\odot}$) and which did not already host an MBH (Sijacki & Springel 2006, Sijacki et al. 2007, Di Matteo et al. 2008, Okamoto et al. 2008, Booth & Schaye 2009, McCarthy et al. 2010). MBHs of a set initial mass (generally $\sim 1 - 5 \times 10^5 M_{\odot}$) are then fixed to the center of the halo, and are allowed to grow through gas accretion and mergers with other MBHs. Some properties of the MBH population are correctly captured by this method, in the sense that they do not depend on the initial mass and formation efficiency of MBHs. For instance the luminosity function of quasars, which measures the properties of the most massive MBHs in the most massive galaxies at any given time, is not very sensitive to the initial properties of the population; these properties may affect only the faint end, which is not well determined observationally. Therefore this strategy works well for understanding the global properties of the evolved population of MBHs at late times, however, this approach is unlikely to capture the physics of MBH formation.

An alternate approach is taken by (Bellovary et al. 2011), who employ a zero-metallicity requirement as well as density and temperature thresholds for MBH formation. If a particle meets density, temperature, and metallicity criteria, it is given a probability of forming an MBH seed. This probability mimics the efficiency of MBH seed formation and can be adjusted freely. As a result of this method, more than one MBH can exist per galaxy, though the most massive ones tend to form early on and remain at the galaxy centers, near the regions of early dense star formation. Fig. 3 exemplifies how this MBH formation model naturally forms MBHs only at high redshift. MBH formation ends when the Universe becomes enriched with heavy elements created by the first generations of stars. Heavy elements have more efficient cooling via line emission, which in turn favors formation of individual stars over the efficient collection of gas conducive to MBH formation.

Adaptive mesh refinement (AMR) simulations use a different approach. In (Dubois et al. 2012) MBHs are spawned from maximally refined regions which are Jeans unstable. These regions must exceed a set gas density threshold as well as a stellar fraction threshold, to ensure that MBHs form from dense gas after the formation of the first

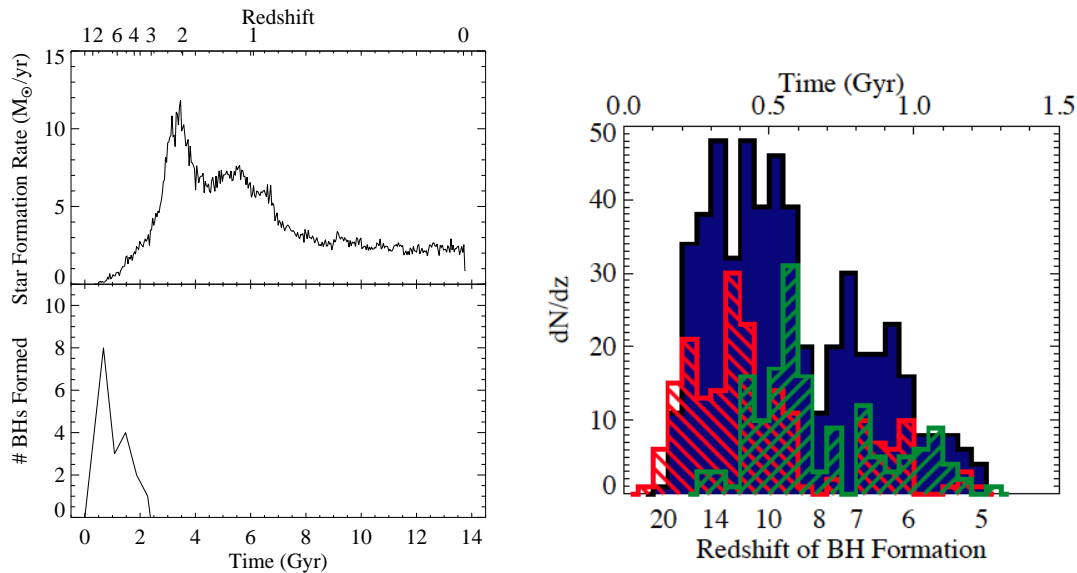


Figure 3. Left: MBH and star formation rates from one of our Milky Way-size galaxy. MBH formation is truncated due to contamination by heavy elements, while stars continue forming. Right: Time of formation of MBHs in a dwarf galaxy (green), a Milky-Way galaxy (red) and a massive elliptical (blue). We can see the trend of earlier onset of MBH formation in the more biased cosmic overdensities. The rate of seed formation dwindles around $z = 5$ because supernova explosions have enriched the Universe with heavy elements. Both panels adapted from Bellovary (2011).

stars. To maintain only one MBH per galaxy, MBHs are not allowed to form within some r_{min} of another MBH.

4.2.2. Accretion. The physical processes which govern the accretion of gas by MBHs take place on scales with size of order the solar system, roughly 12 orders of magnitude smaller than the size of a whole galaxy. It is not surprising then that large-scale simulations of galaxy formation must make assumptions about how gas travels from larger, resolvable scales to the MBH. Phenomena such as angular momentum transfer, magnetic fields, and general relativity must be ignored. Cosmological simulations by (Levine et al. 2010) demonstrated that mass inflow toward an MBH is extremely chaotic on small scales, rendering a broad characterization of large-scale MBH accretion estimates extremely difficult. Still, with some clever sub-grid modeling we can hope to create a basic representation of reality.

The most common approach to modeling MBH accretion is a method based on the Bondi-Hoyle formalism:

$$\dot{M} = \frac{4\pi\alpha G^2 M_{BH}^2 \rho^2}{(c_s^2 + v^2)^{3/2}} \quad (4)$$

where ρ and c_s are the local gas density and sound speed, v is the relative speed between the MBH and the surrounding gas, and α is a dimensionless parameter. The value of α in the precise Bondi-Hoyle formula ranges between 0.25 - 1.12, depending on

the equation of state of the gas. However, simulators have taken this parameter to be extremely flexible, ranging from one (Di Matteo et al. 2008) to 1000 (Sijacki et al. 2007) to a varying function of density (Booth & Schaye 2009). The reason for this variation is due to the inability to resolve the Bondi radius (and thus the high gas densities one expects at this radius). If the gas density at the Bondi radius is underestimated, the MBH’s growth will be artificially stunted. Various authors have adjusted the parameter α such that their cosmological simulations reproduce the local $M - \sigma$ relation and the black hole density evolution over cosmic time.

One can argue that using Bondi-Hoyle accretion as an estimate for the true accretion rate is grossly wrong. Efficient accretion occurs in discs, not spherical systems. While Bondi-Hoyle may be accurate in the case of hot, low density, spherically symmetric gas such as in elliptical galaxies, this case is not a common one and is certainly not the situation when MBHs are accreting most of their mass at high redshift. Indeed, recent simulations show that Bondi-Hoyle accretion is interrupted if a moderate radiation feedback component is introduced (Milosavljević et al. 2009, Barai et al. 2011) (though see (Park & Ricotti 2011) for a solution to this problem involving episodic accretion). While the use of this model may seem questionable, it can also be argued that it is reasonable for the scales which can be resolved in an SPH cosmological simulation. At a distance of a few 100 parsecs from an MBH, any gas which is nearby can be assumed to fall in toward the MBH within a reasonable amount of time. Measuring the gas properties at a large scale can give us a basic estimate of what the accretable gas near the MBH might be like. While we will surely benefit from more sophisticated models in the future, current Bondi-Hoyle models do broadly reflect reality and give us a basic idea of how MBHs interact with the gas in galaxy centers.

More experimentation with MBH accretion has been done in non-cosmological simulations. (Debuhr et al. 2010) developed a viscous disk model of MBH accretion which, when used in idealized simulations of galaxy mergers, reproduces properties of the local $M - \sigma$ relation. Alternatively, (Power et al. 2010) created an “accretion disk particle” which mimics an MBH and its accretion disk. When low angular momentum gas particles come within the disk radius, they are captured and accreted within an accretion timescale. (Dotti et al. 2007) use a simulation of a circumnuclear disc with a resolution of 0.1 pc to study the properties of the gas that gets bound to an MBH. They define weakly bound, bound, and strongly bound particles according to the relationship between the total (sum of the kinetic, internal and gravitational) energy per unit mass, E , and the gravitational potential, W , of the MBH (e.g., strongly bound particles have $E < 0.5W$, weakly bound particles have $E < 0.25W$, bound particles have $E < 0$). They find that dynamical effects, e.g., the tidal field of the MBH, affect the distribution of particles over the duration of their simulations. None of these models have been implemented in a cosmological simulation; interesting future work would be to see how they fare in different galaxy environments, and how the accretion estimates compare to those derived from Bondi-Hoyle.

4.2.3. Feedback Modeling feedback is critical for simulations of MBH evolution, but as in the case of accretion, the actual physical processes involved are completely unresolved. The most common sub-grid model for MBH feedback is an isotropic thermal energy deposition (Di Matteo et al. 2005). If one assumes that a fraction ϵ_r of the mass accreted by the MBH is converted into energy (usually $\epsilon_r = 10\%$), and a fraction ϵ_f of that energy couples to the surrounding gas, the feedback energy deposition rate is equal to

$$\dot{E} = \epsilon_r \epsilon_f \dot{M} c^2 \quad (5)$$

This method of feedback modeling has been used in the majority of cosmological simulations, with a value of $\epsilon_f = 0.01 - 0.15$ (Sijacki et al. 2007, Di Matteo et al. 2008, Booth & Schaye 2009, Bellovary et al. 2010). (Sijacki et al. 2007) employ a second feedback mechanism as well, to represent mechanical feedback on cluster scales with hot buoyant bubbles. Such simulations have had success in reproducing the observed MBH - host scaling relations as well as the black hole space density evolution.

More advanced feedback models are possible in extremely high resolution simulations, but to achieve this one must sacrifice resolution for simulation size. For example, (Jeon et al. 2011) have run a 1 Mpc³ cosmological simulation to $z \sim 10$ which includes radiative feedback effects from Population III stars and MBHs. They are able to include X-ray photoionization heating processes as a result of accretion onto the MBH, and conclude that the growth of MBH seeds from Population III stars is severely hampered by these feedback effects. Some more recent works with AMR simulations have also incorporated more sophisticated forms of feedback models. (Dubois et al. 2012) include the thermal feedback model mentioned earlier in this section, but also invoke mechanical feedback at times when accretion rates drop below 1% of the Eddington rate (to represent a radio jet). With this model, mass, momentum and energy are distributed within a cylinder oriented along the angular momentum axis of the nearby particles.

A model developed by (Kim et al. 2011) utilizes a radiative mode and a mechanical mode of feedback. For the radiative mode, the high resolution of the simulation allows for a full three-dimensional radiative transfer calculation to be done, with the MBH as the emitting source. Photons are emitted with a temperature of 2 keV and are then able to ionize, heat, and exert momentum onto the surrounding gas. For the mechanical mode, mass is periodically injected along a jet axis with a velocity of 6000 km/s. This model is the most highly sophisticated to date and is extremely promising; however a fully self-consistent cosmological simulation including MBH seed formation at high redshift has not yet been done.

4.2.4. Results Cosmological simulations do an excellent job of broadly representing the growth and evolution of MBHs and their host galaxies. Simulated galaxies have realistic star formation histories, and their predicted colors are what we expect to see in observed populations. We can reproduce the MBH - host scaling relations and the

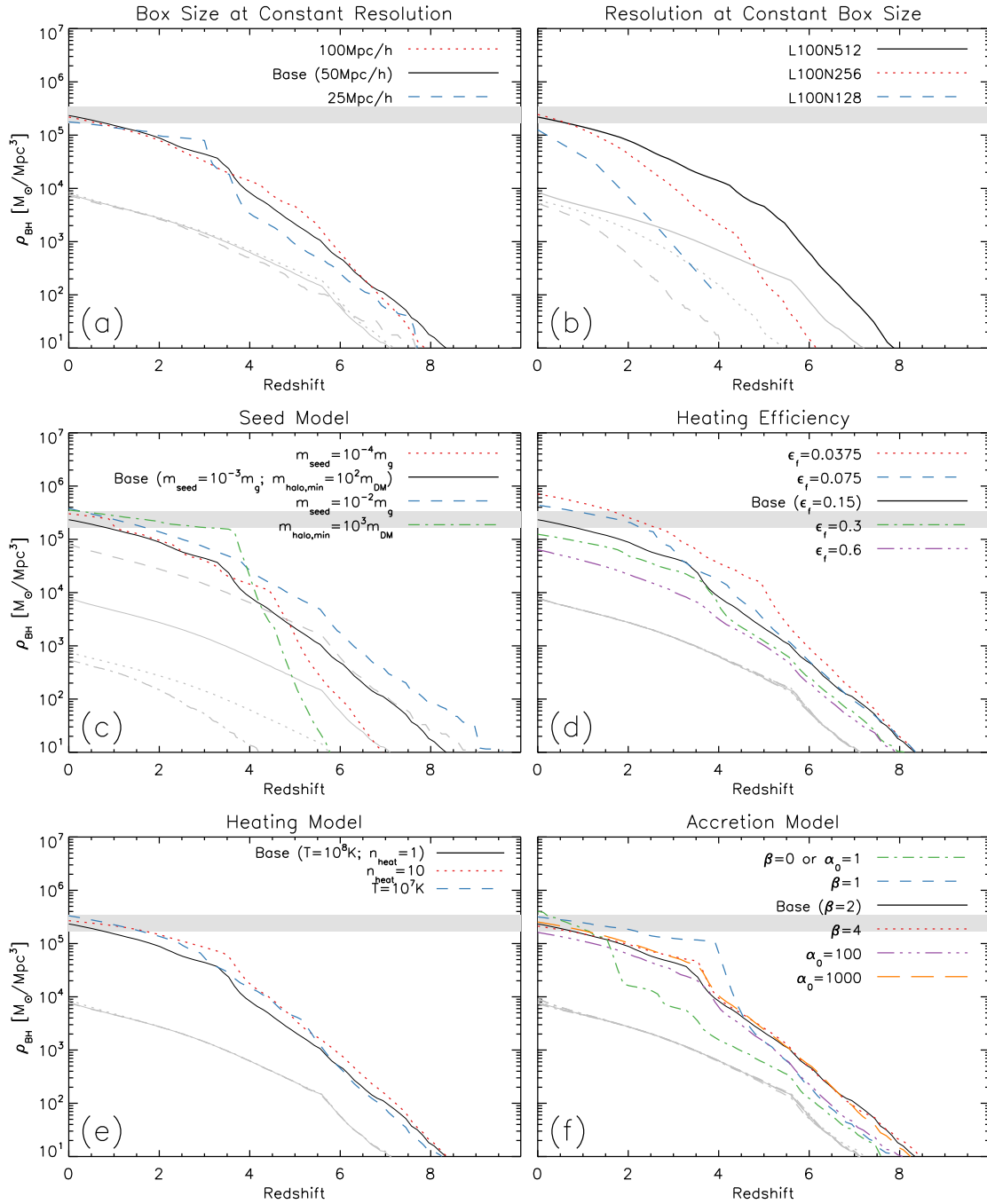


Figure 4. An example parameter study of MBHs in cosmological simulations. Shown here is MBH mass density vs. redshift for a wide range of physical models and parameters. The shaded grey line represents the $z = 0$ value. (Booth & Schaye 2009)

black hole space density at $z = 0$. However, many quantities which are not directly observable are also difficult to quantify in simulations. For example, the MBH mass density is constrained locally (Shankar et al. 2004), but at higher redshifts there are no constraints at all. Varying simulation parameters such as resolution, box size, feedback

efficiency, or accretion models can give different answers at high redshift while agreeing at $z = 0$. This is illustrated in Figure 4, which shows the result of a large parameter space exploration and how the MBH density is affected by varying one at a time. Clearly there are a wide range of “acceptable” models that reproduce the observed $z = 0$ value but vary greatly at higher redshifts.

All in all, cosmological simulations have given us many clues to how MBHs form, grow, and evolve with their host galaxies. The overall picture is fairly clear; MBH seeds form early on in small halos, grow through mergers and gas accretion, and affect their surroundings via feedback. However, the finer details of the physical processes involved are still beyond our reach. Higher resolution simulations and more sophisticated modeling are required in order to answer our remaining questions.

5. Outstanding Questions and Future Developments

There has been much progress to report on the formation and evolution of MBHs, and much more progress will happen in the near future. While many theoretical and observational advances have improved our understanding of how MBHs form and evolve in galaxies, many questions still remain. Theorists have brought forward several models of MBH formation (section 2) but it is very hard to find a direct smoking gun that can pinpoint the right mechanism, or even rule them all out. From the observational point of view we have to rely on secondary indicators (e.g., the occupation fraction of MBHs, their masses in dwarf galaxies, constraints from growth time). From the theoretical point of view, we are either limited to analytical models, or to numerical simulations that can barely resolve the scales where these processes operate, in a well known trade-off between the resolution one can reach and the size of the galaxy one can model.

The co-evolution between galaxies and MBHs is a very active topic of research, and many complementary approaches are likely to provide important clues in the near future. Properties of AGN hosts from local galaxies up to $z \sim 2$ (e.g., SDSS, zCOSMOS) are being coupled with estimates of MBH masses (through line widths (Vestergaard & Peterson 2006)), with more and more attention to possible biases (Kelly et al. 2010). Clever techniques are being used to study not only the most luminous quasars but also less luminous sources (Treister et al. 2011, Mullaney et al. 2012). Ongoing work using integral-field spectroscopy (Davies et al. 2010, Storchi-Bergmann 2010, Müller-Sánchez et al. 2011, Riffel & Storchi-Bergmann 2011) on nearby Seyfert galaxies is revealing spatially resolved distributions and kinematics of the gas that feeds the MBH and fuels star formation. The James Webb Space Telescope and Euclid, successors of the Hubble Space Telescope, and the Atacama Large Millimeter Array will zoom in on the highest quasars, and may eventually bring us to the edge of the Dark Ages when the first MBHs and galaxies formed.

Acknowledgments

MV acknowledges funding support from NASA, through award ATP NNX10AC84G; from SAO, through award TM1-12007X, from NSF, through award AST 1107675, and from a Marie Curie Career Integration grant, PCIG10-GA-2011-303609.

6. References

- Abel T, Bryan G L & Norman M L 2002 *Science* **295**, 93–98.
- Alatalo K, Blitz L, Young L M, Davis T A, Bureau M, Lopez L A, Cappellari M, Scott N, Shapiro K L, Crocker A F, Martín S, Bois M, Bournaud F, Davies R L, de Zeeuw P T, Duc P A, Emsellem E, Falcón-Barroso J, Khochfar S, Krajinović D, Kuntschner H, Lablanche P Y, McDermid R M, Morganti R, Naab T, Oosterloo T, Sarzi M, Serra P & Weijmans A 2011 *ApJ* **735**, 88.
- Alcock C, Allsman R A, Alves D R, Axelrod T S, Becker A C, Bennett D P, Cook K H, Dalal N, Drake A J, Freeman K C, Geha M, Griest K, Lehner M J, Marshall S L, Minniti D, Nelson C A, Peterson B A, Popowski P, Pratt M R, Quinn P J, Stubbs C W, Sutherland W, Tomaney A B, Vandehei T & Welch D 2000 *ApJ* **542**, 281–307.
- Alexander D M, Brandt W N, Smail I, Swinbank A M, Bauer F E, Blain A W, Chapman S C, Coppin K E K, Ivison R J & Menéndez-Delmestre K 2008 *AJ* **135**, 1968–1981.
- Assef R J, Kochanek C S, Ashby M L N, Brodwin M, Brown M J I, Cool R, Forman W, Gonzalez A H, Hickox R C, Jannuzi B T, Jones C, Le Floch E, Moustakas J, Murray S S & Stern D 2011 *ApJ* **728**, 56.
- Balick B & Brown R L 1974 *ApJ* **194**, 265–270.
- Barai P, Proga D & Nagamine K 2011 *MNRAS*, 418, 591.
- Barth A J, Ho L C, Rutledge R E & Sargent W L W 2004 *ApJ* **607**, 90–102.
- Begelman M C 2010 *MNRAS* **402**, 673–681.
- Begelman M C, Rossi E M & Armitage P J 2008 *MNRAS* **387**, 1649–1659.
- Begelman M C & Shlosman I 2009 *ApJL* **702**, L5–L8.
- Begelman M C, Volonteri M & Rees M J 2006 *MNRAS* **370**, 289–298.
- Bellovary J M, Governato F, Quinn T R, Wadsley J, Shen S & Volonteri M 2010 *ApJL* **721**, L148–L152.
- Bellovary J, Volonteri M, Governato F, Shen S, Quinn T & Wadsley J 2011 *ApJ* **742**, 13.
- Bennert V N, Auger M W, Treu T, Woo J H & Malkan M A 2011 *ApJ* **742**, 107.
- Bond J R, Arnett W D & Carr B J 1984 *ApJ* **280**, 825–847.
- Booth C M & Schaye J 2009 *MNRAS* **398**, 53–74.
- Bower R G, Benson A J, Malbon R, Helly J C, Frenk C S, Baugh C M, Cole S & Lacey C G 2006 *MNRAS* **370**, 645–655.
- Bromley B C, Kenyon S J, Geller M J & Brown W R 2012 *ApJL* **749**, L42.
- Bromm V & Larson R B 2004 *ARA&A* **42**, 79–118.
- Bromm V & Loeb A 2003 *ApJ* **596**, 34–46.
- Bundy K, Ellis R S, Conselice C J, Taylor J E, Cooper M C, Willmer C N A, Weiner B J, Coil A L, Noeske K G & Eisenhardt P R M 2006 *ApJ* **651**, 120–141.
- Burkert A & Tremaine S 2010 *ApJ* **720**, 516–521.
- Carr B J 2003 *in* D Giulini, C Kiefer & C Laemmerzahl, eds, ‘Quantum Gravity: From Theory to Experimental Search’ Vol. 631 of *Lecture Notes in Physics*, Berlin Springer Verlag pp. 301–321.
- Ciotti L & Ostriker J P 2007 *ApJ* **665**, 1038–1056.
- Clark P C, Glover S C O, Klessen R S & Bromm V 2011 *ApJ* **727**, 110–+.
- Couchman H M P & Rees M J 1986 *MNRAS* **221**, 53–62.
- Cowie L L, Barger A J & Hasinger G 2012 *ApJ* **748**, 50.
- Cowie L L, Songaila A, Hu E M & Cohen J G 1996 *AJ* **112**, 839–+.

- Croom S M, Richards G T, Shanks T, Boyle B J, Strauss M A, Myers A D, Nichol R C, Pimblett K A, Ross N P, Schneider D P, Sharp R G & Wake D A 2009 MNRAS **399**, 1755–1772.
- Croton D J, Springel V, White S D M, De Lucia G, Frenk C S, Gao L, Jenkins A, Kauffmann G, Navarro J F & Yoshida N 2006 MNRAS **365**, 11–28.
- Davies M B, Miller M C & Bellovary J M 2011 ApJL **740**, L42.
- Davies R I, Hicks E, Schartmann M, Genzel R, Tacconi L J, Engel H, Burkert A, Krause M, Sternberg A, Mueller Sánchez F & Maciejewski W 2010 **267**, 283–289.
- Davies R I, Müller Sánchez F, Genzel R, Tacconi L J, Hicks E K S, Friedrich S & Sternberg A 2007 ApJ **671**, 1388–1412.
- Davies R I, Tacconi L J & Genzel R 2004 ApJ **613**, 781–793.
- Debuhr J, Quataert E, Ma C P & Hopkins P 2010 MNRAS **406**, L55–L59.
- Decarli R, Gavazzi G, Arosio I, Cortese L, Boselli A, Bonfanti C & Colpi M 2007 MNRAS **381**, 136–150.
- Devecchi B & Volonteri M 2009 ApJ **694**, 302–313.
- Devecchi B, Volonteri M, Colpi M & Haardt F 2010 MNRAS **409**, 1057–1067.
- Devecchi B, Volonteri M, Rossi E M, Colpi M & Portegies Zwart S 2012 MNRAS **421**, 1465–1475.
- Di Matteo T, Colberg J, Springel V, Hernquist L & Sijacki D 2008 ApJ **676**, 33–53.
- Di Matteo T, Springel V & Hernquist L 2005 Nature **433**, 604–607.
- Dijkstra M, Haiman Z, Mesinger A & Wyithe J S B 2008 MNRAS **391**, 1961–1972.
- Dotti M, Colpi M, Haardt F & Mayer L 2007 MNRAS **379**, 956–962.
- Dubois Y, Devriendt J, Slyz A & Teyssier R 2012 MNRAS **420**, 2662–2683.
- Eisenstein D J & Loeb A 1995 ApJ **443**, 11–17.
- Fan X, Narayanan V K, Lupton R H, Strauss M A, Knapp G R, Becker R H, White R L, Pentericci L, Leggett S K, Haiman Z, Gunn J E, Ivezić Ž, Schneider D P, Anderson S F, Brinkmann J, Bahcall N A, Connolly A J, Csabai I, Doi M, Fukugita M, Geballe T, Grebel E K, Harbeck D, Hennessy G, Lamb D Q, Miknaitis G, Munn J A, Nichol R, Okamura S, Pier J R, Prada F, Richards G T, Szalay A & York D G 2001 AJ **122**, 2833–2849.
- Ferrarese L & Merritt D 2000 ApJL **539**, L9–L12.
- Feruglio C, Maiolino R, Piconcelli E, Menci N, Aussel H, Lamastra A & Fiore F 2010 AAP **518**, L155.
- Fiore F, Puccetti S, Grazian A, Menci N, Shankar F, Santini P, Piconcelli E, Koekemoer A M, Fontana A, Boutsia K, Castellano M, Lamastra A, Malacaria C, Feruglio C, Mathur S, Miller N & Pannella M 2012 AAP **537**, A16.
- Gallo E, Treu T, Jacob J, Woo J, Marshall P J & Antonucci R 2008 ApJ **680**, 154–168.
- Gebhardt K, Bender R, Bower G, Dressler A, Faber S M, Filippenko A V, Green R, Grillmair C, Ho L C, Kormendy J, Lauer T R, Magorrian J, Pinkney J, Richstone D & Tremaine S 2000 ApJL **539**, L13–L16.
- Glikman E, Djorgovski S G, Stern D, Dey A, Jannuzi B T & Lee K S 2011 ApJL **728**, L26.
- Graham A W & Driver S P 2007 ApJ **655**, 77–87.
- Graham A W & Spitler L R 2009 MNRAS **397**, 2148–2162.
- Greene J E, Peng C Y, Kim M, Kuo C Y, Braatz J A, Violette Impellizzeri C M, Condon J J, Lo K Y, Henkel C & Reid M J 2010 ApJ **721**, 26–45.
- Greif T, Springel V, White S, Glover S, Clark P, Smith R, Klessen R & Bromm V 2011, ApJ, 737, 75
- Gültekin K, Richstone D O, Gebhardt K, Lauer T R, Tremaine S, Aller M C, Bender R, Dressler A, Faber S M, Filippenko A V, Green R, Ho L C, Kormendy J, Magorrian J, Pinkney J & Siopis C 2009 ApJ **698**, 198–221.
- Haiman Z & Loeb A 2001 ApJ **552**, 459–463.
- Håring N & Rix H 2004 ApJL **604**, L89–L92.
- Hawking S 1971 MNRAS **152**, 75–+.
- Heger A & Woosley S E 2002 ApJ **567**, 532–543.
- Hopkins P F, Quataert E & Murray N 2011 MNRAS **417**, 950–973.
- Jeon M, Pawlik A, Greif T H, Glover S, Bromm V, Milosavljevic M & Klessen R S, 2012 ApJ, 754, 34
- Johnson J L & Bromm V 2007 MNRAS **374**, 1557–1568.

- Johnson J L, Greif T H & Bromm V 2008 MNRAS **388**, 26–38.
- Kelly B C, Vestergaard M, Fan X, Hopkins P, Hernquist L & Siemiginowska A 2010, ApJ, 719, 1315
- Khlopov M Y 2010 *Research in Astronomy and Astrophysics* **10**, 495–528.
- Khlopov M Y, Rubin S G & Sakharov A S 2005 *Astroparticle Physics* **23**, 265–277.
- Kim J h, Wise J H, Alvarez M A & Abel T 2011 ApJ **738**, 54.
- Kodama T, Yamada T, Akiyama M, Aoki K, Doi M, Furusawa H, Fuse T, Imanishi M, Ishida C, Iye M, Kajisawa M, Karoji H, Kobayashi N, Komiyama Y, Kosugi G, Maeda Y, Miyazaki S, Mizumoto Y, Morokuma T, Nakata F, Noumaru J, Ogasawara R, Ouchi M, Sasaki T, Sekiguchi K, Shimasaku K, Simpson C, Takata T, Tanaka I, Ueda Y, Yasuda N & Yoshida M 2004 MNRAS **350**, 1005–1014.
- Koushiappas S M, Bullock J S & Dekel A 2004 MNRAS **354**, 292–304.
- Lauer T R, Tremaine S, Richstone D & Faber S M 2007 ApJ **670**, 249–260.
- Levine R, Gnedin N Y & Hamilton A J S 2010 ApJ **716**, 1386–1396.
- Lodato G & Natarajan P 2006 MNRAS **371**, 1813–1823.
- Loeb A & Rasio F A 1994 ApJ **432**, 52–61.
- Madau P & Rees M J 2001 ApJL **551**, L27–L30.
- Magorrian J, Tremaine S, Richstone D, Bender R, Bower G, Dressler A, Faber S M, Gebhardt K, Green R, Grillmair C, Kormendy J & Lauer T 1998 AJ **115**, 2285–2305.
- Marconi A & Hunt L K 2003 ApJL **589**, L21–L24.
- Mayer L, Kazantzidis S, Escala A & Callegari S 2010 Nature **466**, 1082–1084.
- McCarthy I G, Schaye J, Ponman T J, Bower R G, Booth C M, Vecchia C D, Crain R A, Springel V, Theuns T & Wiersma R P C 2010 Mon. Not. R. Astron. Soc. 406 822-839
- McConnell N J, Ma C P, Gebhardt K, Wright S A, Murphy J D, Lauer T R, Graham J R & Richstone D O 2011 Nature **480**, 215–218.
- Merritt D 2009 ApJ **694**, 959–970.
- Miller B, Gallo E, Treu T & Woo J H 2012 ApJ **747**, 57.
- Milosavljević M, Bromm V, Couch S M & Oh S P 2009 ApJ **698**, 766–780.
- Monaco P, Theuns T & Taffoni G 2002 MNRAS **331**, 587–608.
- Mullaney J R, Daddi E, Béthermin M, Elbaz D, Juneau S, Pannella M, Sargent M T, Alexander D M & Hickox R C 2012, ApJ, 753, 30
- Müller-Sánchez F, Prieto M A, Hicks E K S, Vives-Arias H, Davies R I, Malkan M, Tacconi L J & Genzel R 2011 ApJ **739**, 69.
- Murray N, Quataert E & Thompson T A 2005 ApJ **618**, 569–585.
- Nesvadba N P H, Lehnert M D, De Breuck C, Gilbert A M & van Breugel W 2008 AAP **491**, 407–424.
- Oh S P & Haiman Z 2002 ApJ **569**, 558–572.
- Okamoto T, Nemmen R S & Bower R G 2008 Mon. Not. R. Astron. Soc. 385 161-180
- Omukai K, Schneider R & Haiman Z 2008 ApJ **686**, 801–814.
- Oppenheimer B D & Davé R 2008 MNRAS **387**, 577–600.
- Page D N & Hawking S W 1976 ApJ **206**, 1–7.
- Park K & Ricotti M 2011 ApJ **739**, 2.
- Peng C Y, Impey C D, Rix H W, Kochanek C S, Keeton C R, Falco E E, Lehár J & McLeod B A 2006 ApJ **649**, 616–634.
- Power C, Nayakshin S & King A Power C, Nayakshin S and King A 2010 Mon. Not. R. Astron. Soc. 412 269-276
- Reines A E, Sivakoff G R, Johnson K E & Brogan C L 2011 Nature **470**, 66–68.
- Ricotti M, Ostriker J P & Mack K J 2008 ApJ **680**, 829–845.
- Riffel R A & Storchi-Bergmann T 2011 MNRAS **417**, 2752–2769.
- Sadoun R & Colin J 2012 *ArXiv e-prints*, arXiv:1204.0144 .
- Sarria J E, Maiolino R, La Franca F, Pozzi F, Fiore F, Marconi A, Vignali C & Comastri A 2010 AAP **522**, L3.
- Schawinski K, Thomas D, Sarzi M, Maraston C, Kaviraj S, Joo S J, Yi S K & Silk J 2007 MNRAS

- 382**, 1415–1431.
- Schawinski K, Virani S, Simmons B, Urry C M, Treister E, Kaviraj S & Kushkuley B 2009 *ApJL* **692**, L19–L23.
- Seth A, Agüeros M, Lee D & Basu-Zych A 2008 *ApJ* **678**, 116–130.
- Shang C, Bryan G L & Haiman Z 2010 *MNRAS* **402**, 1249–1262.
- Shankar F, Salucci P, Granato G L, De Zotti G & Danese L 2004 *MNRAS* **354**, 1020–1030.
- Sijacki D & Springel V 2006 *MNRAS* **366**, 397–416.
- Sijacki D, Springel V, di Matteo T & Hernquist L 2007 *MNRAS* **380**, 877–900.
- Silk J 2011 *in* C. Carignan, F. Combes, & K. C. Freeman, ed., ‘IAU Symposium’ Vol. 277 of *IAU Symposium* pp. 273–281.
- Silk J & Rees M J 1998 *A&A* **331**, L1–L4.
- Springel V, White S D M, Jenkins A, Frenk C S, Yoshida N, Gao L, Navarro J, Thacker R, Croton D, Helly J, Peacock J A, Cole S, Thomas P, Couchman H, Evrard A, Colberg J & Pearce F 2005 *Nature* **435**, 629–636.
- Stacy A, Greif T H & Bromm V 2012 *Mon. Not. R. Astron. Soc.* **422** 290–309
- Storchi-Bergmann T 2010 *in* ‘IAU Symposium’ Vol. 267 of *IAU Symposium* pp. 290–298.
- Targett T A, Dunlop J S & McLure R J 2012 *MNRAS* **420**, 3621–3631.
- Tisserand P, Le Guillou L, Afonso C, Albert J N, Andersen J, Ansari R, Aubourg É, Bareyre P, Beaulieu J P, Charlot X, Coutures C, Ferlet R, Fouqué P, Glicenstein J F, Goldman B, Gould A, Graff D, Gros M, Haissinski J, Hamadache C, de Kat J, Lasserre T, Lesquoy É, Loup C, Magneville C, Marquette J B, Maurice É, Maury A, Milsztajn A, Moniez M, Palanque-Delabrouille N, Perdureau O, Rahal Y R, Rich J, Spiro M, Vidal-Madjar A, Vigroux L, Zylberajch S & The EROS-2 Collaboration 2007 *AAP* **469**, 387–404.
- Treister E, Schawinski K, Volonteri M, Natarajan P & Gawiser E 2011 *Nature* **474**, 356–358.
- Tremaine S, Gebhardt K, Bender R, Bower G, Dressler A, Faber S M, Filippenko A V, Green R, Grillmair C, Ho L C, Kormendy J, Lauer T R, Magorrian J, Pinkney J & Richstone D 2002 *ApJ* **574**, 740–753.
- Tremonti C A, Moustakas J & Diamond-Stanic A M 2007 *ApJL* **663**, L77–L80.
- Treu T, Ellis R S, Liao T X & van Dokkum P G 2005 *ApJL* **622**, L5–L8.
- Turk M J, Abel T & O’Shea B 2009 *Science* **325**, 601–.
- van Wassenhove S, Volonteri M, Walker M G & Gair J R 2010 *Mon. Not. R. Astron. Soc.* **408** 1139–1146
- Vestergaard M & Peterson B M 2006 *ApJ* **641**, 689–709.
- Volonteri M & Begelman M C 2010 *Mon. Not. R. Astron. Soc.* **409** 1022–1032
- Volonteri M, Dotti M, Campbell D & Mateo M 2011 *ApJ* **730**, 145.
- Volonteri M, Haardt F & Madau P 2003 *ApJ* **582**, 559–573.
- Volonteri M, Lodato G & Natarajan P 2008 *MNRAS* **383**, 1079–1088.
- Volonteri M & Stark D P 2011 *MNRAS* **417**, 2085–2093.
- Wild V, Heckman T & Charlot S 2010 *MNRAS* **405**, 933–947.
- Willott C J 2011 *ApJL* **742**, L8.
- Willott C J, Delorme P, Reylé C, Albert L, Bergeron J, Crampton D, Delfosse X, Forveille T, Hutchings J B, McLure R J, Omont A & Schade D 2010 *AJ* **139**, 906–918.
- Woo J H, Treu T, Malkan M A & Blandford R D 2008 *ApJ* **681**, 925–930.
- Yan R, Ho L C, Newman J A, Coil A L, Willmer C N A, Laird E S, Georgakakis A, Aird J, Barmby P, Bundy K, Cooper M C, Davis M, Faber S M, Fang T, Griffith R L, Koekemoer A M, Koo D C, Nandra K, Park S Q, Sarajedini V L, Weiner B J & Willner S P 2011 *ApJ* **728**, 38–+.
- Zel’Dovich Y B & Novikov I D 1967 *Soviet Astronomy* **10**, 602–+.